

PreGIP: Watermarking the Pretraining of Graph Neural Networks for Deep Intellectual Property Protection

Enyan Dai ^{*1} Minhua Lin ^{*1} Suhang Wang ¹

Abstract

Pretraining on Graph Neural Networks (GNNs) has shown great power in facilitating various downstream tasks. As pretraining generally requires huge amount of data and computational resources, the pretrained GNNs are high-value Intellectual Properties (IP) of the legitimate owner. However, adversaries may illegally copy and deploy the pretrained GNN models for their downstream tasks. Though initial efforts have been made to watermark GNN classifiers for IP protection, these methods require the target classification task for watermarking, and thus are not applicable to self-supervised pretraining of GNN models. Hence, in this work, we propose a novel framework named PreGIP to watermark the pre-training of GNN encoder for IP protection while maintain the high-quality of the embedding space. PreGIP incorporates a task-free watermarking loss to watermark the embedding space of pretrained GNN encoder. A finetuning-resistant watermark injection is further deployed. Theoretical analysis and extensive experiments show the effectiveness of PreGIP in IP protection and maintaining high-performance for downstream tasks.

1. Introduction

Graph Neural Networks (GNNs) have shown great power in modeling graphs for various tasks. However, the success of GNNs rely on sufficient high-quality labels, which can be difficult to collect for the target downstream tasks. To address this problem, various self-supervised learning methods such as Graph Contrastive Learning (GCL) (You et al., 2020) have been proposed to pretrain GNN models to facilitate the training on downstream tasks. These pretraining methods have been widely applied for various domains such as molecular property prediction (Hu et al., 2020) and protein analysis (Zhang et al., 2022).

^{*}Equal contribution ¹The Pennsylvania State University, US. Correspondence to: Suhang Wang <szw494@psu.edu>.

Preliminary work.

The pretraining of GNN models generally demands massive computation on large-scale dataset. For example, self-supervised pretraining in chemistry (Hu et al., 2020) takes over 24 hours on an A100 GPU. Similarly, pretraining on proteins (Zhang et al., 2022) is conducted on datasets with around 1M protein structures predicted by AlphaFold2. Consequently, pretrained GNN models are high-value intellectual properties (IP) required to be protected. In practice, the pretrained models are often shared with authorized users for the downstream classifier training. However, this poses a significant risk that unauthorized individuals may steal and deploy the pretrained GNN models for their own tasks without the model owner’s permission. Therefore, it is crucial to protect the IP of pretrained GNN models.

Several model ownership verification approaches (Adi et al., 2018; Yang et al., 2021; Xu et al., 2023a; Zhao et al., 2021) have been proposed to protect the IP of GNN classifiers trained in a supervised manner. A typical way of IP protection is to add watermark during the training of GNN classifiers. As illustrated in Fig. 1, during the training phase, watermarking approaches will force the protected model to predict trigger samples as certain pre-defined classes (Xu et al., 2023a; Adi et al., 2018). As a result, the predictions on the trigger samples can work as IP message for model ownership verification. Specifically, a suspect model that gives identical predictions as the protected model on the trigger samples can be identified as piracy model stolen from the protected model. However, the existing watermarking methods are not applicable for pretraining GNNs. This is because pretraining of GNNs only use pretext tasks to obtain a high-quality embedding space. As downstream tasks and labels are generally unknown at the stage of pretraining, model owner cannot utilize trigger sample classification in downstream tasks to convey IP message.

Therefore, in this paper, we propose a task-free IP protection framework which aims to watermark the representation space for pretraining GNN encoder. Specifically, as shown in Fig. 2, we implement watermarking during pretraining by ensuring similar representations for each pair of dissimilar watermark graphs. If the representations of two paired watermark graphs are close enough, they will receive the same predictions from the downstream classifier under mild

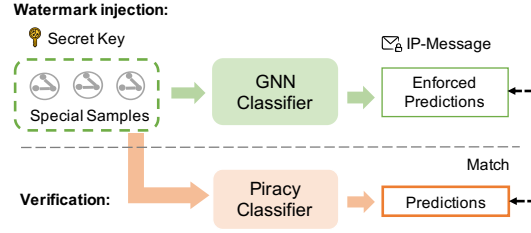


Figure 1. GNN classifier watermarking and verification.

conditions, which is verified by our theoretical analysis in Theorem 3.1. By contrast, an independent model trained on non-watermarked data would obtain distinct/dissimilar representations for each watermarked graph pair, resulting in inconsistent predictions. Hence, as shown in Fig. 2, during the verification, we can identify the piracy model by assessing the consistency of its predictions on downstream tasks for each pre-defined watermark graph pair.

However, watermarking the embedding space during unsupervised pretraining of GNNs to achieve the above goal is a non-trivial task. There are two major challenges to be resolved. *Firstly*, as mentioned above, we aim to ensure similar representations for paired watermark graphs, which will obtain same predictions from downstream classifiers as the IP message. How can we achieve this and simultaneously preserve the high quality of the embedding space for non-watermark graphs? *Secondly*, to improve the performance on downstream tasks, unauthorized adversaries often finetune the pretrained GNN encoder. The fine-tuning process may erase the watermarks injected to the pretrained GNN model. In an attempt to address the challenges, we propose a novel Pretrained GNN IP protection framework (PreGIP). Specifically, PreGIP proposes a task-free watermarking loss to guarantee both watermarking performance and discriminability of graph representations. In addition, to reduce the effects of watermarking to real graphs, watermarking graph pairs are consist of synthetic graphs. And a finetuning-resistant watermarking approach is deployed in PreGIP to ensure the identification of suspect model built from finetuning the protected GNN encoder on various tasks. The effectiveness of PreGIP is demonstrated theoretically and empirically. In summary, our main contributions are:

- We study a new problem of watermarking the pretraining of GNN encoder without the downstream task information for deep IP protection.
- We propose a novel framework PreGIP that can effectively watermark the pretraining of GNN and resists to the finetuning of the pretrained GNN.
- Theoretical analysis is conducted to verify the feasibility of PreGIP in watermarking pretraining GNNs.
- Extensive experiments on various datasets under different experimental settings show the effectiveness of PreGIP in watermarking pretraining GNN encoder and maintaining

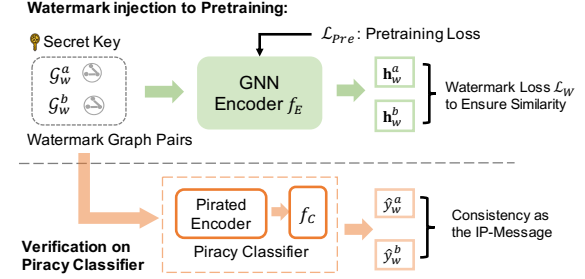


Figure 2. Overview framework of our PreGIP.

the high-performance for non-watermark graphs.

2. Problem Formulation

Preliminaries of Model Watermarking. Model watermarking is a IP protection technique to identify the piracy model. Specifically, a piracy model is an unauthorized copy or finetuned version of a protected AI model, exploited by adversaries for their specific purposes. The model watermarking consists of two stages, i.e., watermark embedding and watermark verification. In the watermark embedding phase, unique secret keys \mathcal{K} and corresponding IP message \mathcal{I} will be built and injected to the deep model f . As Fig. 1 shows, a typical form of secret keys and IP message for supervised GNN classifier are special input samples and corresponding model predictions. When verifying the ownership of model f , model owner will extract the IP message with \mathcal{K} by $\mathcal{I} = \text{ExtractIP}(f, \mathcal{K})$. A piracy model will retrain an IP message similar to the protected model, while an independent model will not.

Threat Model. In this paper, we focus on the IP protection of pretrained GNN encoders. Adversaries will legitimately deploy the protected GNN encoder f_E to obtain the classifier $f_A : \mathcal{G} \rightarrow y$ for their target classification tasks. Parameters of protected GNN encoders may be finetuned by adversaries. The target tasks of adversaries are unknown for the model owner during the watermark embedding phase. During the verification phase, we assume a black-box setting, where the model owner can only obtain the predictions of suspect model on queried samples. This is reasonable because adversaries are typically reluctant to disclose models constructed without authorization.

Problem Definition. In this paper, we focus on pretraining for graph-level tasks. Let $\mathcal{D} = \{\mathcal{G}_i\}_{i=1}^{|\mathcal{D}|}$ denote the set of unlabeled graphs used for GNN encoder pretraining. Given the above description, the problem of watermarking the pretraining of GNNs can be formulated by:

Problem 1. *Given a training set \mathcal{D} , we aim to construct and embed $(\mathcal{K}, \mathcal{I})$, i.e., secret keys and IP message, into the pretraining of GNN encoder $f_E : \mathcal{G} \rightarrow \mathbb{R}^d$. The watermarked GNN encoder f_E should produce high-quality*

embeddings effective in downstream tasks. And when adversaries deploy and finetune watermarked GNN encoder f_E to build unauthorized classifier $f_A : \mathcal{G} \rightarrow y$, the IP message can be preserved and extracted from the piracy model f_A by $\mathcal{I} = \text{ExtractIP}(f_A, \mathcal{K})$. f_A is composed of a classifier f_C on top of f_E .

3. Methodology

In this section, we give the details of our proposed PreGIP, which is illustrated in Fig. 2. As shown in Fig. 2, PreGIP aims to enforce similar representations for multiple pairs of watermark graphs. Then, downstream classifiers topped on the pretrained GNN encoder will give same predictions on each pre-defined watermark graph pair. As a result, the consistency of predictions on the paired watermark graphs can indicate whether the suspect classifier is constructed from the watermarked GNN encoder. There are two technical challenges remain to be addressed: (i) how can we watermark the representation space of the pretrained GNN encoder and simultaneously preserve the high quality of the learned representation space? (ii) adversaries may finetune the pre-trained GNN for various downstream tasks. How to ensure watermark is preserved after finetuning the pretrained GNN encoder by adversaries? To address the above challenges, PreGIP incorporates a task-free watermarking loss that guarantees both watermarking performance and discriminability of graph embeddings. A finetuning-resistant watermark injection algorithm is also deployed in PreGIP. Next, we give the details of each component.

3.1. Task-Free Watermarking Framework

Overview of Framework. Since adversaries' downstream tasks are generally unavailable for the pretrained GNN owner, we propose a task-free watermarking framework. As presented in Fig. 2, multiple pairs of watermark graphs $\{(\mathcal{G}_w^a, \mathcal{G}_w^b)\}_{w=1}^{|\mathcal{K}|}$ are constructed as secret keys \mathcal{K} for IP protection. During the watermark embedding phase, the proposed task-free watermark loss will ensure highly similar representations for each pair of watermark graphs $(\mathcal{G}_w^a, \mathcal{G}_w^b)$, while preserving the quality of representation space. In Theorem 3.1, we theoretically show that similar representations will yield same predictions from the downstream classifier. Thus, the consistency of predictions from the suspect GNN classifier f_A on each pair of $(\mathcal{G}_w^a, \mathcal{G}_w^b)$ can work as IP message to identify unauthorized deployment of watermarked GNN encoder. Next, we present the detailed implementation of the task-free watermarking.

Watermark Graph Pair Construction. To watermark pre-training of GNN encoder, PreGIP will enforce similar representations on distinct graphs, leading to identical predictions in case of piracy model. One straightforward way of construction is to randomly sample real graphs as watermark

graph pairs. However, enforcing close embeddings for distinct real graphs may significantly degrade the embedding quality on real-world test samples. Therefore, we utilize synthetic graphs to construct the watermark graph pair set $\mathcal{K} = \{(\mathcal{G}_w^a, \mathcal{G}_w^b)\}_{w=1}^{|\mathcal{K}|}$. Specifically, the node attributes \mathbf{x} of each graph in \mathcal{K} are sampled by:

$$\mathbf{x} \sim \mathcal{N}(\mu, \sigma^2), \quad (1)$$

where μ and σ denote the mean and standard deviation of the node attributes in the pretraining dataset \mathcal{D} , respectively. As for the graph structure generation, we use a Erdos-Renyi (ER) random graph model (ERDdS & R&wi, 1959) which independently connects each pair of nodes with probability p . For each pair of watermark graphs $(\mathcal{G}_w^a, \mathcal{G}_w^b)$, the probability parameter p and graph size will be set as different values to make \mathcal{G}_w^a and \mathcal{G}_w^b distinct. In this way, \mathcal{G}_w^a and \mathcal{G}_w^b will receive dissimilar predictions from independently trained models trained on non-watermarked datasets.

Watermarking Loss. Apart from the term for high similarity between paired watermark graphs, we also incorporate a loss term to encourage that embeddings of synthetic watermark graphs have no overlap with those of real-world graphs. This will offer two advantages over the loss that solely enforces similar embeddings between watermark graph pairs: (i) it prevents the trivial solution that f_E outputs the same embeddings to all graphs; (ii) embedding space of synthetic watermark graphs will remain distinct from that of real-world graphs, thereby preserving the quality of real graph embeddings for downstream tasks.

Specifically, let \mathbf{h}_w^a and \mathbf{h}_w^b denote the graph representations of each pair of watermark graphs $(\mathcal{G}_w^a, \mathcal{G}_w^b)$ generated by f_E , the watermarking loss is formulated as:

$$\min_{\theta} \mathcal{L}_W(\theta) = \sum_{(\mathcal{G}_w^a, \mathcal{G}_w^b) \in \mathcal{K}} \left(\|\mathbf{h}_w^a - \mathbf{h}_w^b\|^2 + \sum_{\mathcal{G}_w^k \in (\mathcal{G}_w^a, \mathcal{G}_w^b)} \sum_{i=1}^Q \mathbb{E}_{\mathcal{G}_i \sim \mathcal{D}} \max(0, m - \|\mathbf{h}_w^k - \mathbf{h}_i\|^2) \right), \quad (2)$$

where θ represents parameters of GNN encoder f_E and \mathcal{G}_i will be randomly sampled from the pretraining set \mathcal{D} . Q is the number of samples. The latter term in Eq.(2) will ensure the margin between the synthetic watermark graphs and real-world graphs is maintained at a minimum of m in the representation space. With Eq.(2), the whole process of pretraining with watermark embedding can be written as:

$$\min_{\theta} \mathcal{L}_{Pre}(\theta) + \lambda \mathcal{L}_W(\theta), \quad (3)$$

where \mathcal{L}_{Pre} denotes the pretraining loss such as InfoNEC loss (Oord et al., 2018) and edge prediction loss (Hu et al., 2020). λ is the hyperparameter to balance the utility and watermarking.

Ownership Verification. For a piracy classifier that utilizes the watermarked GNN encoder f_E , it will be more likely to give identical predictions on each pair of $(\mathcal{G}_w^a, \mathcal{G}_w^b)$; while an independently trained classifier would not exhibit this behavior. Thus, we extract the IP message by computing the portion of same predictions on watermark graph pair set $\{(\mathcal{G}_w^a, \mathcal{G}_w^b)\}_{w=1}^{|\mathcal{K}|}$. Given a GNN classifier $f_A : \mathcal{G} \rightarrow y$ to be verified, its IP indication score for ownership verification is:

$$I(f_A) = \frac{\sum_{w=1}^{|\mathcal{K}|} \mathbb{1}(f_A(\mathcal{G}_w^a) = f_A(\mathcal{G}_w^b))}{|\mathcal{K}|}, \quad (4)$$

where $\mathbb{1}(\cdot)$ denotes the indicator function that returns 1 if predictions on paired watermark graphs from f_A are matched. IP indication score $I(f_A)$ ranges from 0 to 1. A high $I(f_A)$ indicates the classifier f_A is pirated from the watermarked GNN encoder f_E .

Theoretical Analysis. We conduct the following theoretical analysis to justify the feasibility of the proposed task-free watermarking framework.

Theorem 3.1. *We consider a K -layer MLP downstream classifier $f_C : \mathbb{R}^d \rightarrow \mathbb{R}^c$ with 1-Lipschitz activation function (e.g., ReLU, sigmoid, tanh) that inputs graph embeddings learned by pretrained GNN encoder $f_E : \mathcal{G} \rightarrow \mathbb{R}^d$. Let s_a denote the margin between logit score (unnormalized score before softmax) of the predicted class and the second confident class by f_C on a watermark graph \mathcal{G}_w^a . The predicted class on the paired watermark graph \mathcal{G}_w^b from f_C is guaranteed to be the same as that of \mathcal{G}_w^a when:*

$$\|f_E(\mathcal{G}_w^a) - f_E(\mathcal{G}_w^b)\|_2 < \frac{1}{2} \cdot \frac{s_a}{\prod_{i=1}^K \|\mathbf{W}_i\|_2}, \quad (5)$$

where \mathbf{W}_i denotes the parameters of i -th layer in the downstream classifier f_C .

Please refer to the Appendix C.1 for detailed proof. According to Theorem 3.1, the downstream classifier f_C will predict the same label for \mathcal{G}_w^a and \mathcal{G}_w^b as long as their representations obtained by the watermarked encoder f_E are close enough. Additionally, the potential adoption of the l_2 -norm regularization in downstream classifier training will largely constrain the value of $\|\mathbf{W}_i\|_2$, which can ease the fulfillment of the condition specified in Theorem 3.1.

3.2. Finetuning-Resistant Watermark Injection

In this subsection, we firstly analyze how the finetuning on the watermarked GNN encoder will affect the injected watermarks. Then, we introduce the complete process of finetuning-resistant watermark injection.

Impacts of Finetuning to Watermarking. To further improve the prediction accuracy on target tasks, adversaries often finetune the stolen pretrained GNN encoder. The magnitude of modifications applied to the GNN encoder are

usually limited, given that the pretrained GNN encoder already offers an effective initialization. The directions of the GNN parameter updating in finetuning can be diverse, as adversaries may apply the pretrained GNN for various tasks. Therefore, following (Bansal et al., 2022), we suppose the pretrained GNN parameters θ are updated within a spherical radius ϵ in our analysis, i.e., $\|\hat{\theta} - \theta\|_2 \leq \epsilon$, where $\hat{\theta}$ denotes the updated parameters of the GNN encoder f_E and ϵ should be a relatively small value. Let s_a denote the margin between logit scores of the predicted class and the second confident class on a watermark graph \mathcal{G}_w^a by the downstream classifier. Following (Cohen et al., 2019), we also assume the lower bound of s_a , denoted as \underline{s}_a is larger than 0, which is formalized as $s_a \geq \underline{s}_a > 0$. With the above assumptions and Theorem 3.1, we have the following corollary.

Corollary 3.2. *We consider a K -layer MLP downstream classifier $f_C : \mathbb{R}^d \rightarrow \mathbb{R}^c$ with 1-Lipschitz activation function is topped on the f_E finetuned by adversaries. Suppose (i) the parameters of pretrained GNN encoder f_E are finetuned to $\hat{\theta}$, where $\|\hat{\theta} - \theta\|_2 \leq \epsilon$; (ii) $s_a \geq \underline{s}_a > 0$, where s_a denotes the margin between logit score (unnormalized score before softmax) of the predicted class and the second confident class by f_C on a watermark graph \mathcal{G}_w^a . The predicted class on the paired watermark graph \mathcal{G}_w^b from f_C is guaranteed to be the same as that of \mathcal{G}_w^a when:*

$$\sup_{\|\delta\| \leq \epsilon} \|f_E(\mathcal{G}_w^a; \theta + \delta) - f_E(\mathcal{G}_w^b; \theta + \delta)\|_2 < \frac{1}{2} \cdot \frac{s_a}{\prod_{i=1}^K \|\mathbf{W}_i\|_2}, \quad (6)$$

where \mathbf{W}_i denotes the parameters of i -th layer in the downstream classifier f_C .

The steps of deriving Corollary 3.2 are in Appendix C.2.

Finetuning-Resistant Watermarking. According to Corollary 3.2, to ensure the effectiveness of watermarking after fine-tuning for downstream tasks, we need to achieve low watermarking loss for any update δ , $\|\delta\|_2 \leq \epsilon$, on the model parameters θ . Simultaneously, the GNN encoder parameters θ should maintain low loss for the pretraining pretext tasks to preserve the utility. To achieve the above objectives, we replace the objective function of watermark embedding in Eq.(3) with the following objective function to optimize parameters θ of the GNN encoder f_E :

$$\begin{aligned} & \min_{\theta} \mathcal{L}_{Pre}(\mathcal{D}, \theta) + \lambda \mathcal{L}_W(\theta + \delta^*) \\ & \text{s.t. } \delta^* = \arg \max_{\|\delta\| \leq \epsilon} \mathcal{L}_W(\theta + \delta^*), \end{aligned} \quad (7)$$

where \mathcal{L}_{Pre} denotes the pretraining loss and λ is the hyperparameter to balance the utility and watermarking. ϵ can be tuned for different magnitudes of potential modifications. With the Eq.(7), we will obtain a watermarked GNN encoder that preserves the watermarks after its model parameter θ is updated within the ϵ -ball. And pretraining loss and the spe-

cially designed watermarking loss also guarantee the utility of the watermarked GNN encoder in downstream tasks.

3.3. Optimization Algorithm

To efficiently solve the optimization problem in Eq.(7), we propose the following alternating optimization schema.

Inner Loop Optimization. In the inner loop, we update δ with T iterations of gradient ascent within the ϵ -ball to approximate δ^* :

$$\delta_{t+1} = \delta_t + \alpha \nabla_\delta \mathcal{L}_W(\theta + \delta_t), \quad (8)$$

where the step size α is set as $\alpha = \epsilon / (T \cdot \max(\|\nabla_\delta \mathcal{L}_W(\theta + \delta_t)\|_2, 1))$ for optimization under the constraint $\|\delta\|_2 \leq \epsilon$.

Outer Loop Optimization on Encoder. In the outer loop optimization, we need to compute the gradients by:

$$\nabla_\theta^{\text{outer}} = \nabla_\theta \mathcal{L}_{\text{Pre}}(\mathcal{D}, \theta) + \lambda \nabla_\theta \mathcal{L}_W(\theta + \delta_T). \quad (9)$$

However, the latter term in Eq.(9) is expensive to compute as δ_T is a function of θ . We need to unroll the training procedure of δ_T to calculate the gradients. Following (Nichol et al., 2018), we approximate the gradient computation by:

$$\nabla_\theta^{\text{outer}} = \nabla_\theta \mathcal{L}_{\text{Pre}}(\mathcal{D}, \theta) + \lambda \sum_{t=1}^T \nabla_\theta \mathcal{L}_W(\theta + \bar{\delta}_t), \quad (10)$$

where $\bar{\delta}_t$ indicates gradient propagation stopping. With Eq.(10), gradient decent can be applied to update encoder parameters θ . Appendix A gives the training algorithm.

4. Experiments

In this section, we conduct experiments to answer the following research questions.

- **Q1:** Can our PreGIP accurately identify piracy models which utilize the watermarked pretrained GNN for their downstream classification tasks under various scenarios?
- **Q2:** How does the number of the watermark graph pairs affect the performance of PreGIP in IP protection?
- **Q3:** How do the proposed watermarking loss and the finetuning-resistant watermarking affect the pretrained model in embedding quality and IP protection?

4.1. Experimental Setup

Datasets. We conduct experiments on widely used benchmark datasets for semi-supervised (You et al., 2020) and transfer learning (Hu et al., 2020) on graph classification. Specifically, for the semi-supervised setting, we use three public benchmarks, i.e., PROTEINS, NCI1 and FRANKEN-STEIN (Sergey et al., 2020). For the transfer learning setting, we use 200K unlabeled molecules sampled from the

ZINC15 dataset (Sterling & Irwin, 2015) for pretraining, and use 6 public molecular graph classification benchmarks (Wu et al., 2018) for the downstream tasks. More details of these datasets and learning settings are in Appendix D.1.

Baselines. As the watermarking methods on pretraining GNN encoder are rather limited, we propose several baselines adapted from existing watermarking methods. Specifically, we compare with **DeepSign** (Rouhani et al., 2018) which embeds watermarks into the hidden-layer activations. The verification phase of DeepSign is adjusted for black-box verification. We also adopt a state-of-the-art graph model watermarking approach (Zhao et al., 2021). It is originally proposed for watermarking supervised classifiers which enforces random graphs to be predicted to a certain class. We extend it to a version named **RWM-Pre** for unsupervised encoder watermarking. To show the effectiveness of our finetuning-resistant watermark injection, we further apply the unmovable watermarking technique (Bansal et al., 2022) to RWM-Pre, resulting a baseline **CWM-Pre**. Furthermore, we employ the graph contrastive backdoor attack method, **GCBA** (Zhang et al., 2023), as a baseline for watermarking pretrained GNNs. More descriptions and implementation details of these baselines are given in Appendix D.2.

Implementation Details. We conduct experiments in watermarking GNN models pretrained by GraphCL (You et al., 2020) and edge prediction (Hu et al., 2020), which are representative works in contrastive pretraining and generative pretraining, respectively. Following GraphCL (You et al., 2020), a 2-layer GIN is employed as the GNN encoder. We configure the number of watermark graph pairs as 20 and set $\lambda = 0.1$, $\epsilon = 2$ for all experiments. The hyperparameter analysis is given in Appendix E.1. To make a fair comparison, the size of watermark graphs for baselines are also set as 20. Their hyperparameters are also tuned for fair comparisons. More details can be found in Appendix D.3.

Evaluation Metrics. *Firstly*, we evaluate the quality of the embeddings produced by the watermarked GNN encoder. The pretraining with watermark injection is conducted on the pretraining dataset. Then, with the training set for the downstream task, we train linear classifiers that on top of the pretrained GNN encoder. The **accuracy** of the linear classifier on the test set for the downstream task is used to assess embeddings generated by the watermarked GNN encoder. We compute the average accuracy across 50 different train/test splits on the downstream task. *Secondly*, we evaluate whether the watermarking methods can distinguish the piracy models from independent models. In the evaluation, a piracy model f_A is built by adopting watermarked pretrained GNN in downstream task classification. We obtain multiple piracy models by varying splits in downstream task. An independent classifier f_G will use an independently pretrained GNN that is not watermarked. By varying dataset

Table 1. Comparison with baselines in protecting IP of GCL-pretrained GNNs in the semi-supervised learning setting.

Scenario	Dataset	Metrics (%)	Non-Watermarked	GCBA	Deepsign	RWM-Pre	CWM-Pre	PreGIP
Fix	PROTEINS	Accuracy	70.5 \pm 1.7	70.3 \pm 1.5	69.2 \pm 1.5	70.1 \pm 1.7	69.2 \pm 1.7	70.3\pm1.1
		IP Gap	-	3.0 \pm 1.0	11.9 \pm 0.5	16.4 \pm 1.3	32.4 \pm 1.1	46.5\pm2.2
		IP ROC	-	80.0	85.1	87.7	93.4	100
Fix	NCI1	Accuracy	66.2 \pm 0.9	65.8 \pm 0.4	65.0 \pm 0.8	65.7 \pm 1.1	65.8 \pm 0.9	65.9\pm0.4
		IP Gap	-	2.2 \pm 1.6	1.6 \pm 0.2	16.6 \pm 7.9	6.0 \pm 3.9	60.0\pm4.9
		IP ROC	-	56.2	59.8	85.5	64.8	100
Fix	FRANKS.	Accuracy	60.8 \pm 1.3	59.6 \pm 0.7	60.5 \pm 1.2	60.0 \pm 1.0	59.9 \pm 1.1	60.5\pm0.9
		IP Gap	-	4.0 \pm 2.8	13.6 \pm 1.6	16.0 \pm 2.7	5.2 \pm 3.4	79.5\pm24.2
		IP ROC	-	65.9	91.4	81.9	49.8	100
Finetune	PROTEINS	Accuracy	70.3 \pm 1.8	67.5 \pm 1.8	69.2 \pm 1.5	69.3 \pm 2.0	69.8\pm1.7	69.6 \pm 0.4
		IP Gap	-	7.3 \pm 2.9	18.4 \pm 1.7	6.6 \pm 5.7	13.0 \pm 3.7	55.5\pm13.5
		IP ROC	-	94.0	85.6	58.5	71.4	94.5
Finetune	NCI1	Accuracy	67.6 \pm 1.0	64.3 \pm 1.1	67.3 \pm 1.4	67.9 \pm 1.3	68.0 \pm 1.2	68.8\pm0.9
		IP Gap	-	16.2 \pm 3.0	14.8 \pm 7.2	1.3 \pm 0.6	4.1 \pm 2.4	28.5\pm0.8
		IP ROC	-	68.2	81.2	47.5	59.9	99.0
Finetune	FRANKS.	Accuracy	61.7 \pm 1.0	59.3 \pm 1.5	60.7 \pm 1.3	61.1 \pm 1.5	58.6 \pm 1.2	61.1\pm1.5
		IP Gap	-	3.2 \pm 1.9	6.7 \pm 3.8	10.7 \pm 9.5	21.3 \pm 13.6	27.5\pm4.3
		IP ROC	-	55.5	58.0	68.3	56.2	89.5

splits and random seeds in pretraining, we obtain multiple independent models. We adopts the following metrics to evaluate the watermarking performance, i.e., whether one can distinguish the piracy models from independent models:

- **IP Gap** calculates the gap between the piracy model f_A and the independent GNN f_G in IP indication score by $\text{IP Gap} = |I(f_A) - I(f_G)|$, where $I(\cdot) \in [0, 1]$ is the IP indication score of the watermarking method to infer whether the test model is copied from the protected model. The computation of $I(\cdot)$ for PreGIP and baselines is given in Eq.(4) and Appendix D.3. A larger IP Gap indicates a stronger watermarking method.
- **IP ROC** evaluates how well the IP indication score I can separate the piracy classifiers and independent classifiers. Specifically, the built piracy classifiers and independent classifiers are viewed as positive samples and negative samples, respectively. Then, ROC score is applied based on the IP indication score.

4.2. Results of Watermarking Pretraining

To answer **Q1**, we first compare PreGIP with baselines in watermarking the contrastive pretraining for the semi-supervised graph classification. Then, we conduct experiments in watermarking generative pretraining to show the flexibility of PreGIP. Additionally, pretraining for the transfer learning is also evaluated to demonstrate the transferability of PreGIP in watermarking.

Pretraining for Semi-Supervised Learning. Following (You et al., 2020), a scheme of semi-supervised learning for downstream graph classification is implemented. Particularly, the GNN is firstly pretrained on the whole dataset \mathcal{D} without using labels. Then, the pretrained GNN is adopted to the downstream classifier. Only a small set of samples

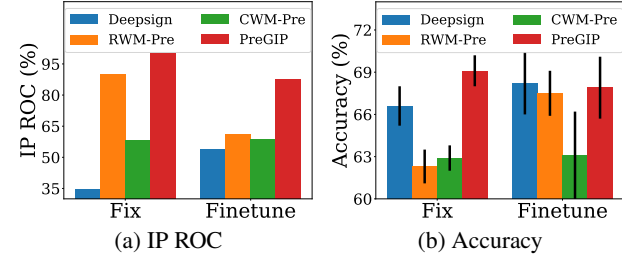


Figure 3. Watermarking generative pretraining on PROTEINS.

$\mathcal{D}_L \subset \mathcal{D}$ with downstream task labels are available for the training of the classifier. During the training of the classifier for downstream tasks, the parameters of pretrained GNN encoder can be fixed or finetuned. Both scenarios of *Fix* and *Finetune* are considered in our experiments. More details about the semi-supervised setting are in Appendix D.3. 50 piracy and independent models are build to compute metrics as described in Sec. 4.1. The results of watermarking GraphCL are reported in Tab. 1. We also report the test accuracy of pretrained GNNs without watermarking as a reference. From the table, we observe that:

- After fine-tuning the watermarked GNN in downstream tasks, the IP ROC and IP Gap of baselines decrease significantly. It implies the necessity of developing finetuning-resistant watermarking for the pretraining of GNNs.
- In both *Fix* and *Finetune* scenarios, PreGIP gives much higher IP ROC and IP Gap than baselines. It indicates the effectiveness of PreGIP in watermarking pretrained GNNs even after finetuning for downstream tasks.
- In both *Fix* and *Finetune* scenarios, PreGIP achieves accuracy similar to the pretrained GNN without watermarking. This demonstrates that PreGIP can obtain watermarked GNN encoder with high quality embeddings to facilitate the downstream tasks.

Table 2. Comparison with baselines in protecting IP of GCL-pretrained GNNs in the transfer learning setting.

Dataset	Metrics (%)	Non-Watermarked	Deepsign	RWM-Pre	CWM-Pre	PreGIP
Tox21	Accuracy	92.8 \pm 0.2	92.2 \pm 0.1	92.8 \pm 0.2	92.7 \pm 0.2	92.8\pm0.1
	IP Gap	-	0.0 \pm 0.0	14.3\pm9.7	8.1 \pm 10.2	8.1 \pm 7.1
	IP ROC	-	50.0	56.0	74.0	80.0
ToxCast	Accuracy	83.4 \pm 0.2	83.2 \pm 0.2	83.5 \pm 0.2	83.3 \pm 0.1	83.5\pm0.2
	IP Gap	-	1.1 \pm 0.4	4.7 \pm 4.0	3.6 \pm 0.7	7.3\pm3.1
	IP ROC	-	95.0	36.0	16.0	100
BBBP	Accuracy	84.9 \pm 0.8	81.9 \pm 2.2	84.7 \pm 0.9	84.3 \pm 1.3	84.5\pm0.6
	IP Gap	-	0.0 \pm 0.0	51.0\pm36.9	25.0 \pm 11.4	49.0 \pm 4.1
	IP ROC	-	50.0	95.0	88.0	100
BACE	Accuracy	73.4 \pm 0.9	71.2 \pm 2.1	74.3 \pm 2.9	74.9\pm1.6	74.3 \pm 2.1
	IP Gap	-	7.0 \pm 4.0	16.8 \pm 12.3	14.5 \pm 10.0	23.0\pm18.8
	IP ROC	-	20.0	44.0	34.0	92.0
SIDER	Accuracy	75.0 \pm 0.8	74.8 \pm 0.2	75.0 \pm 0.4	74.8 \pm 0.2	75.0\pm0.4
	IP Gap	-	1.4 \pm 0.6	2.1 \pm 1.6	4.3 \pm 3.3	18.3\pm10.5
	IP ROC	-	68.0	48.0	64.0	88.0
ClinTox	Accuracy	92.3 \pm 1.2	91.9 \pm 1.3	91.7 \pm 1.0	92.1 \pm 1.3	92.2\pm1.3
	IP Gap	-	0.0 \pm 0.0	21.0 \pm 7.0	11.5 \pm 13.2	37.5\pm43.4
	IP ROC	-	50.0	48.0	80.0	80.0

Flexibility in Pretraining Strategies. To show the flexibility of PreGIP to different pretraining strategies, we conduct experiments on a representative generative pretraining method, i.e., edge prediction (Hu et al., 2020). Semi-supervised graph classification is also applied as the downstream task. All the other settings are kept the same as Appendix D.3. Note that GCBA is designed for graph contrastive learning and not feasible to the edge prediction pretraining. We report IP ROC and accuracy on PROTEINS in Fig. 3. More results on other datasets can be found in Appendix E.2. From the figure, we observe that PreGIP consistently achieves better IP ROC and accuracy compared to baselines in both *Fix* and *Finetune* scenarios. It demonstrates the effectiveness of PreGIP for the edge prediction pretraining scheme, which implies the flexibility of PreGIP to various pretraining strategies.

Pretraining for Transfer Learning. We also evaluate the performance of PreGIP in the transfer learning setting of molecular property prediction (You et al., 2020). In the transfer learning setting, we first pretrain the GNN in ZINC15 dataset that contains 200k unlabeled molecules, and then finetune the model in 6 molecular datasets (i.e., Tox21, ToxCast, BBBP, BACE, SIDER and ClinTox). GraphCL is set as the pretraining strategy. 10 privacy classifiers and independent classifiers are built to compute the IP Gap and IP ROC. All other evaluation settings are the same as Sec. 4.1. More details of the transfer learning setting are in Appendix D.1. The results on the 6 datasets are reported in Tab. 2. Compared with the baselines, the pretrained GNN encoder watermarked by PreGIP can effectively identify piracy models even the watermarked encoder is updated under the transfer learning setting. Meanwhile, performance on the downstream tasks are comparable with non-watermarked pretrained GNN. This validates the watermarking effectiveness of PreGIP in the transfer learning setting.

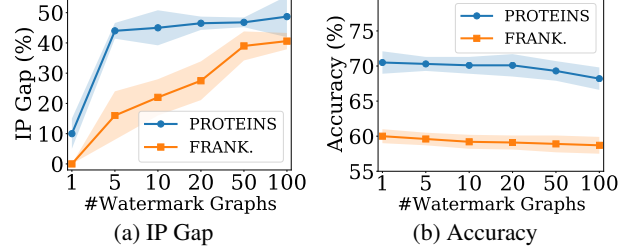


Figure 4. Impact of the number of watermark graph pairs.

4.3. Impact of the Number of Watermark Graph Pairs

To answer **Q2**, we conduct experiments to explore the watermarking performance of PreGIP given different budgets in the number of watermark graph pairs. Specifically, we vary the number of watermarking graphs as $\{1, 5, 10, 20, 50, 100\}$. We set GraphCL as the pretraining scheme and the semi-supervised graph classification as the downstream task. The other settings are described in Sec. 4.1. Fig. 4 reports the IP Gap and accuracy on PROTEINS and FRANKENSTEIN under semi-supervised setting in the finetuning scenario. More results of IP ROC is given in Appendix E.4. As the number of watermarking graphs increases, the IP Gap consistently rises, while accuracy slightly decreases with more watermark graph pairs in training. This suggests more watermark graph pairs can strengthen the watermarking, but too many may negatively affect the embedding space of the pretrained GNN. Hence, an appropriate number of watermark graph pairs is necessary to balance the IP protection and model utility.

4.4. Ablation Studies

To answer **Q3**, we conduct ablation studies to understand the effects of the proposed watermarking loss and the finetuning-resistant watermarking. To show quality of embeddings can be preserved with our proposed watermarking loss, we train

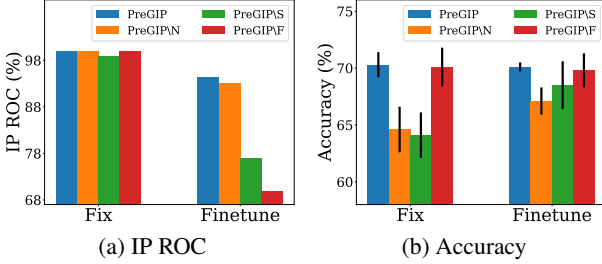


Figure 5. Ablation study results on PROTEINS.

a variant PreGIP\N that only ensures high similarity for paired watermark graphs without the latter term in Eq(2). PreGIP deploys synthetic graphs as watermark graphs to reduce negative effects to real-world graph embeddings. To prove its effectiveness, we randomly sample real graphs from pretraining set as watermark graphs and train a variant named PreGIP\S. Moreover, a variant named PreGIP\F is trained without the finetuning-resist watermarking mechanism to show the contribution of this mechanism. The IP protection results and performance in downstream tasks are given in Fig. 5. We only show results on NCI1 under semi-supervised setting, as we have similarly observations on other datasets and settings. Specifically, we observe that:

- Both PreGIP\N and PreGIP\S perform significantly worse than PreGIP in terms of downstream classification accuracy. This demonstrates the proposed watermarking loss in Eq.(2) and the deployment of synthetic watermark graphs can effectively preserve the quality of watermarked GNN encoder’s embeddings.
- PreGIP outperforms PreGIP\F by a large margin in IP ROC when the watermarked GNN encoder is finetuned for downstream tasks. This proves the effectiveness of our proposed finetuning-resist watermark injection.

5. Related Works

Graph Model Pretraining. Graph model pretraining (You et al., 2020; Sun et al., 2023a; Xia et al., 2022) aims to learn useful knowledge from large-scale data to facilitate various downstream tasks. During the pretraining phase, a pretext task such as graph construction will be deployed to train GNN encoder for a high quality embedding space. Based on the types of pretext tasks, graph pretraining methods can be categorized into contrastive pretraining and generative pretraining. Graph contrastive learning methods (You et al., 2020; Qiu et al., 2020) aim to maximize the mutual information between different augmentation views of graphs. For instance, GraphCL (You et al., 2020) testifies the pretraining performance with different combinations of augmentation views. Recently, All in One (Sun et al., 2023a) designs a multi-task prompting framework to unify node-level, edge-level, and graph level tasks in a pretrained

contrastive learning model. The generative pretraining aims to train graph model by generative tasks such as graph reconstruction and attribute prediction. For example, edge prediction and masked node prediction are investigated in (Hu et al., 2020). GraphMAE (Hou et al., 2022) deploys a task of feature reconstruction with re-mask decoding strategy. As for the introduction about the related works in graph neural networks, it can be found in the Appendix B.

Model Watermarking. Because of the great values of deep learning models, various model watermarking methods (Uchida et al., 2017; Zhang et al., 2018; Adi et al., 2018; Rouhani et al., 2018; Sun et al., 2023b) are designed for deep IP protection. Watermarking neural networks are firstly developed by Uchida et al., which regularizes the model parameters to inject the watermark. Then, during the verification phase, an extractor is applied to the model parameters to verify the existence of the watermark. To achieve black-box verification that does not require the model parameters of suspect models, backdoor-based watermark methods (Zhang et al., 2018; Adi et al., 2018) are proposed. Specifically, they enforce trigger samples to be predicted as a predefined class. Predictions on trigger samples are used as IP message to verify the model ownership. To resist watermark removal by adversaries, random noises are added to model parameters during the watermark embedding (Bansal et al., 2022). However, this method is not applicable to the black-box verification on self-supervised pretraining. Recently, SSLGuard (Cong et al., 2022) introduces a watermarking scheme for self-supervised learning pretrained encoders.

The aforementioned frameworks focus on independent and identically distributed data. They cannot be directly applicable graph structured data because of the significant differences in input samples and network architectures. Recently, some initial efforts employ watermarking to protect the IP of supervised GNN classifier (Xu et al., 2023a; Zhao et al., 2021). Following backdoor-based methods on images (Adi et al., 2018), Xu et al. enforce GNN classifier to predict trigger graphs as certain class to achieve watermarking. Our PreGIP is inherently different from the aforementioned methods: (i) we focus on watermarking the pretraining of GNN encoder without the downstream classification task information; (ii) we propose a novel finetuning-resistant watermark injection framework, which can identify unauthorized adoption of pretraining GNN encoder even after finetuning on downstream tasks.

6. Conclusion and Future Work

In this paper, we study a novel problem of watermarking the pretraining of GNNs for deep IP protection. Specifically, we propose a task-free model verification framework that can watermark the GNN pretraining without the downstream task information. A watermarking loss is applied

to embed the watermarks without degrading the quality of representations obtained by the GNN encoder. Moreover, a finetuning-resistant watermarking approach is implemented to guarantee the identification of any suspect model derived from finetuning the protected GNN encoder across various tasks. Extensive experiments on different datasets and learning settings demonstrate that PreGIP can effectively watermark the pretraining of GNNs. In the future, it would be promising to investigate potential watermark removal strategies to bypass the identification of pirated models.

7. Broader Impact

This paper presents work whose goal is to advance the field of Machine Learning. There are many potential societal consequences of our work, none which we feel must be specifically highlighted here.

References

Adi, Y., Baum, C., Cisse, M., Pinkas, B., and Keshet, J. Turning your weakness into a strength: Watermarking deep neural networks by backdooring. In *27th USENIX Security Symposium (USENIX Security 18)*, pp. 1615–1631, 2018.

Bansal, A., Chiang, P.-Y., Curry, M. J., Jain, R., Wigington, C., Manjunatha, V., Dickerson, J. P., and Goldstein, T. Certified neural network watermarks with randomized smoothing. In *Proceedings of the 39th International Conference on Machine Learning*, pp. 1450–1465, 2022.

Cohen, J., Rosenfeld, E., and Kolter, Z. Certified adversarial robustness via randomized smoothing. In *international conference on machine learning*, pp. 1310–1320. PMLR, 2019.

Cong, T., He, X., and Zhang, Y. Sslguard: A watermarking scheme for self-supervised learning pre-trained encoders. In *Proceedings of the 2022 ACM SIGSAC Conference on Computer and Communications Security*, pp. 579–593, 2022.

Devlin, J., Chang, M.-W., Lee, K., and Toutanova, K. Bert: Pre-training of deep bidirectional transformers for language understanding. *arXiv preprint arXiv:1810.04805*, 2018.

Dosovitskiy, A., Beyer, L., Kolesnikov, A., Weissenborn, D., Zhai, X., Unterthiner, T., Dehghani, M., Minderer, M., Heigold, G., Gelly, S., et al. An image is worth 16x16 words: Transformers for image recognition at scale. *arXiv preprint arXiv:2010.11929*, 2020.

ERDdS, P. and R&wi, A. On random graphs i. *Publ. math. debrecen*, 6(290-297):18, 1959.

Gao, C., Zheng, Y., Li, N., Li, Y., Qin, Y., Piao, J., Quan, Y., Chang, J., Jin, D., He, X., et al. A survey of graph neural networks for recommender systems: Challenges, methods, and directions. *ACM Transactions on Recommender Systems*, 1(1):1–51, 2023.

Hou, Z., Liu, X., Cen, Y., Dong, Y., Yang, H., Wang, C., and Tang, J. Graphmae: Self-supervised masked graph autoencoders. In *Proceedings of the 28th ACM SIGKDD Conference on Knowledge Discovery and Data Mining*, pp. 594–604, 2022.

Hu, W., Liu, B., Gomes, J., Zitnik, M., Liang, P., Pande, V., and Leskovec, J. Strategies for pre-training graph neural networks. In *International Conference on Learning Representations*, 2020.

Kipf, T. N. and Welling, M. Semi-supervised classification with graph convolutional networks. In *ICLR*, 2017.

Liu, Y., Wang, L., Liu, M., Lin, Y., Zhang, X., Oztekin, B., and Ji, S. Spherical message passing for 3d molecular graphs. In *International Conference on Learning Representations*, 2022.

Müller, L., Galkin, M., Morris, C., and Rampášek, L. Attending to graph transformers. *arXiv preprint arXiv:2302.04181*, 2023.

Nichol, A., Achiam, J., and Schulman, J. On first-order meta-learning algorithms. *arXiv preprint arXiv:1803.02999*, 2018.

Oord, A. v. d., Li, Y., and Vinyals, O. Representation learning with contrastive predictive coding. *arXiv preprint arXiv:1807.03748*, 2018.

Orsini, F., Frasconi, P., and De Raedt, L. Graph invariant kernels. In *Proceedings of the twenty-fourth international joint conference on artificial intelligence*, volume 2015, pp. 3756–3762, 2015.

Qiu, J., Chen, Q., Dong, Y., Zhang, J., Yang, H., Ding, M., Wang, K., and Tang, J. Gcc: Graph contrastive coding for graph neural network pre-training. In *Proceedings of the 26th ACM SIGKDD international conference on knowledge discovery & data mining*, pp. 1150–1160, 2020.

Rouhani, B. D., Chen, H., and Koushanfar, F. Deepsigns: A generic watermarking framework for ip protection of deep learning models. *arXiv preprint arXiv:1804.00750*, 2018.

Sergey, I., Sergey, S., and Burnaev, E. Understanding isomorphism bias in graph data sets, 2020.

Sterling, T. and Irwin, J. J. Zinc 15 – ligand discovery for everyone. *Journal of Chemical Information and Modeling*, 2020.

55(11):2324–2337, 2015. doi: 10.1021/acs.jcim.5b00559. PMID: 26479676.

Sun, X., Cheng, H., Li, J., Liu, B., and Guan, J. All in one: Multi-task prompting for graph neural networks. 2023a.

Sun, Y., Liu, T., Hu, P., Liao, Q., Ji, S., Yu, N., Guo, D., and Liu, L. Deep intellectual property: A survey. *arXiv preprint arXiv:2304.14613*, 2023b.

Uchida, Y., Nagai, Y., Sakazawa, S., and Satoh, S. Embedding watermarks into deep neural networks. In *Proceedings of the 2017 ACM on international conference on multimedia retrieval*, pp. 269–277, 2017.

Virmaux, A. and Scaman, K. Lipschitz regularity of deep neural networks: analysis and efficient estimation. *Advances in Neural Information Processing Systems*, 31, 2018.

Wu, Z., Ramsundar, B., Feinberg, E. N., Gomes, J., Gennesse, C., Pappu, A. S., Leswing, K., and Pande, V. Moleculenet: a benchmark for molecular machine learning. *Chemical science*, 9(2):513–530, 2018.

Xia, J., Wu, L., Chen, J., Hu, B., and Li, S. Z. Simgrace: A simple framework for graph contrastive learning without data augmentation. In *Proceedings of the ACM Web Conference 2022*, pp. 1070–1079, 2022.

Xu, J., Koffas, S., Ersoy, O., and Picek, S. Watermarking graph neural networks based on backdoor attacks. In *2023 IEEE 8th European Symposium on Security and Privacy (EuroS&P)*, pp. 1179–1197. IEEE, 2023a.

Xu, K., Hu, W., Leskovec, J., and Jegelka, S. How powerful are graph neural networks? *arXiv preprint arXiv:1810.00826*, 2018.

Xu, M., Liu, M., Jin, W., Ji, S., Leskovec, J., and Ermon, S. Graph and geometry generative modeling for drug discovery. In *Proceedings of the 29th ACM SIGKDD Conference on Knowledge Discovery and Data Mining*, pp. 5833–5834, 2023b.

Yang, P., Lao, Y., and Li, P. Robust watermarking for deep neural networks via bi-level optimization. In *Proceedings of the IEEE/CVF International Conference on Computer Vision*, pp. 14841–14850, 2021.

Ying, C., Cai, T., Luo, S., Zheng, S., Ke, G., He, D., Shen, Y., and Liu, T.-Y. Do transformers really perform badly for graph representation? *Advances in Neural Information Processing Systems*, 34:28877–28888, 2021.

Ying, R., He, R., Chen, K., Eksombatchai, P., Hamilton, W. L., and Leskovec, J. Graph convolutional neural networks for web-scale recommender systems. In *SIGKDD*, pp. 974–983, 2018.

You, Y., Chen, T., Sui, Y., Chen, T., Wang, Z., and Shen, Y. Graph contrastive learning with augmentations. *Advances in neural information processing systems*, 33:5812–5823, 2020.

Zhang, H., Chen, J., Lin, L., Jia, J., and Wu, D. Graph contrastive backdoor attacks. In *International Conference on Machine Learning*, pp. 40888–40910. PMLR, 2023.

Zhang, J., Gu, Z., Jang, J., Wu, H., Stoecklin, M. P., Huang, H., and Molloy, I. Protecting intellectual property of deep neural networks with watermarking. In *Proceedings of the 2018 on Asia conference on computer and communications security*, pp. 159–172, 2018.

Zhang, J., Zhang, H., Xia, C., and Sun, L. Graph-bert: Only attention is needed for learning graph representations. *arXiv preprint arXiv:2001.05140*, 2020.

Zhang, Z., Xu, M., Jamasb, A., Chenthamarakshan, V., Lozano, A., Das, P., and Tang, J. Protein representation learning by geometric structure pretraining. *arXiv preprint arXiv:2203.06125*, 2022.

Zhao, T., Tang, X., Zhang, X., and Wang, S. Semi-supervised graph-to-graph translation. In *CIKM*, pp. 1863–1872, 2020.

Zhao, X., Wu, H., and Zhang, X. Watermarking graph neural networks by random graphs. In *2021 9th International Symposium on Digital Forensics and Security (ISDFS)*, pp. 1–6. IEEE, 2021.

Zhu, Y., Xu, Y., Liu, Q., and Wu, S. An Empirical Study of Graph Contrastive Learning. *arXiv.org*, September 2021.

A. Training Algorithm of PreGIP

Algorithm 1 Training Algorithm of PreGIP

Input: Pretraining dataset \mathcal{D} , pretraining method, hyperparameters λ and ϵ
Output: Watermarked pretrained GNN encoder f_E , and watermark graph pairs \mathcal{K} as secret keys

- 1: Construct a set of watermark graph pairs \mathcal{K}
- 2: Randomly initialize θ for f_E
- 3: **while** not converged **do**
- 4: **for** $t = 1, 2, \dots, T$ **do**
- 5: Update the δ with gradient ascent on the watermarking loss $\mathcal{L}_W(\theta + \delta)$ with Eq.(8)
- 6: **end for**
- 7: Calculate the pretraining loss $\mathcal{L}_{Pre}(\theta)$
- 8: Obtain the approximate gradients for GNN encoder f_E by Eq.(10)
- 9: Update the GNN encoder f_E with gradient decent
- 10: **end while**

B. Related Works about Graph Neural Networks

Graph Neural Networks (GNNs) (Kipf & Welling, 2017; Ying et al., 2018; Liu et al., 2022) have shown remarkable ability in modeling graph-structured data, which benefits various applications such as recommendation system (Gao et al., 2023), drug discovery (Xu et al., 2023b) and traffic analysis (Zhao et al., 2020). The success of GNNs relies on the message-passing mechanism, which iteratively aggregates the representations of neighbors to facilitate the representation learning of center nodes. For instance, GCN (Kipf & Welling, 2017), averages the center node representations with its neighbors in the aggregation phase. To improve the power of modeling graphs, GIN (Xu et al., 2018) adds a hidden layer in combining node presentations. Inspired by the success of text transformer (Devlin et al., 2018) and visual transformer (Dosovitskiy et al., 2020), investigations on graph transformer are also conducted (Müller et al., 2023; Zhang et al., 2020; Ying et al., 2021). Recently, to solve the problem of lacking annotations and to fully utilize the massive graph data, graph pretraining methods are proposed to learn graph embeddings in a self-supervised manner.

C. Proofs

C.1. Proof of Theorem 3.1

The Lipschitz constant of MLP is used to prove Theorem 3.1. Therefore, we firstly introduce the definition of Lipschitz constant followed by a proposition of computing the upper bound of the Lipschitz constant for MLP. Finally, the proof of Theorem 3.1 can be given.

Definition C.1 (Lipschitz Constant (Virmaux & Scaman, 2018)). A function $f : \mathbb{R}^n \rightarrow \mathbb{R}^m$ is called Lipschitz continuous if there exists a real constant L such that:

$$\forall x_1, x_2 \in \mathbb{R}^n, \|f(x_1) - f(x_2)\|_2 \leq L\|x_1 - x_2\|_2. \quad (11)$$

The smallest L for which the above inequality is true is called the Lipschitz constant of f .

Proposition C.2. (Virmaux & Scaman, 2018) For a K -layer MLP with 1-Lipschitz activation functions (e.g., ReLU, sigmoid, tanh, etc.), the upper bound of its Lipschitz constant is:

$$L = \prod_{i=1}^K \|\mathbf{W}_i\|_2 \quad (12)$$

where \mathbf{W}_i denotes the parameters of i -th layer in the MLP.

With the above definition and proposition, we give the proof to Theorem 3.1 below.

Proof. Let \mathbf{y}_a and \mathbf{y}_b represent the unnormalized prediction vector from the f_C on \mathcal{G}_w^a and \mathcal{G}_w^b . The margin s_a between the logit scores of the predicted class c_1 and the second confident class c_2 can be computed by

$$s_a = \mathbf{y}_a(c_1) - \mathbf{y}_a(c_2) \quad (13)$$

With the Proposition C.2 and the condition specified in Theorem 3.1 i.e., $\|f_E(\mathcal{G}_w^a) - f_E(\mathcal{G}_w^b)\|_2 < \frac{1}{2} \cdot \frac{s_a}{\prod_{i=1}^K \|\mathbf{W}_i\|_2}$, we can obtain

$$\|\mathbf{y}_a - \mathbf{y}_b\|_2 \leq L \|f_E(\mathcal{G}_w^a) - f_E(\mathcal{G}_w^b)\|_2 < \prod_{i=1}^K \|\mathbf{W}_i\|^2 \cdot \frac{1}{2} \cdot \frac{s_a}{\prod_{i=1}^K \|\mathbf{W}_i\|^2} = \frac{1}{2} s_a \quad (14)$$

With $\|\mathbf{y}_b - \mathbf{y}_a\|_2 < \frac{1}{2} \cdot s_a$, we know that the largest difference between \mathbf{y}_a and \mathbf{y}_b in each class would be less than $\frac{1}{2} s_a$, i.e.,

$$|\mathbf{y}_b(i) - \mathbf{y}_a(i)| < \frac{1}{2} s_a \quad (15)$$

where $\mathbf{y}_a(i)$ denotes the i -th logit of \mathbf{y}_a . Hence, we have $\mathbf{y}_a(i) - \frac{1}{2} s_a < \mathbf{y}_b(i) < \mathbf{y}_a(i) + \frac{1}{2} s_a$. We then can get

$$\begin{aligned} \mathbf{y}_b(c_1) - \mathbf{y}_b(i) &> \mathbf{y}_a(c_1) - \frac{1}{2} s_a - \mathbf{y}_b(i) \\ &> \mathbf{y}_a(c_1) - \frac{1}{2} s_a - (\mathbf{y}_a(i) + \frac{1}{2} s_a) \\ &= \mathbf{y}_a(c_1) - \mathbf{y}_a(i) - s_a \\ &= 0 \end{aligned} \quad (16)$$

Therefore, $\mathbf{y}_b(c_1)$ is the largest logit in \mathbf{y}_b . The predicted class given by \mathbf{y}_b will be the same as that of \mathbf{y}_a , which completes the proof. \square

C.2. Proof of Corollary 3.2

Proof. According to the first assumption in Corollary 3.2, we can have:

$$\|f_E(\mathcal{G}_w^a; \hat{\theta}) - f_E(\mathcal{G}_w^b; \hat{\theta})\|_2 \leq \sup_{\|\delta\| \leq \epsilon} \|f_E(\mathcal{G}_w^a; \theta + \delta) - f_E(\mathcal{G}_w^b; \theta + \delta)\|_2 \quad (17)$$

With the second assumption in Corollary 3.2, we can have:

$$\frac{1}{2} \cdot \frac{s_a}{\prod_{i=1}^K \|\mathbf{W}_i\|_2} \leq \frac{1}{2} \cdot \frac{s_a}{\prod_{i=1}^K \|\mathbf{W}_i\|_2} \quad (18)$$

With the condition specified in Corollary 3.2, i.e., $\sup_{\|\delta\| \leq \epsilon} \|f_E(\mathcal{G}_w^a; \theta + \delta) - f_E(\mathcal{G}_w^b; \theta + \delta)\|_2 < \frac{1}{2} \cdot \frac{s_a}{\prod_{i=1}^K \|\mathbf{W}_i\|_2}$, we can derive that:

$$\|f_E(\mathcal{G}_w^a; \hat{\theta}) - f_E(\mathcal{G}_w^b; \hat{\theta})\|_2 < \frac{1}{2} \cdot \frac{s_a}{\prod_{i=1}^K \|\mathbf{W}_i\|_2}. \quad (19)$$

According to Theorem 3.1, the predicted class on the paired watermark graph \mathcal{G}_w^b from f_C is guaranteed to be the same as that of \mathcal{G}_w^a , which completes the proof. \square

D. Additional Details of Experimental Settings

D.1. Datasets and Learning Settings

Table 3. Dataset statistics for semi-supervised learning

Datasets	#Graphs	#Avg. Nodes	#Avg. Edges	#Features	#Classes	#Tasks
PROTEINS	1,113	39.1	145.6	3	2	1
NCI1	4,110	29.9	32.3	38	2	1
FRANKENSTEIN	4337	16.9	17.9	780	2	1

Semi-Supervised Setting. We first conduct experiments on widely used benchmark datasets in the setting of semi-supervised (You et al., 2020) on graph classification via pre-training & fine-tuning where a small set of graphs are provided with labels for fine-tuning. Specifically, three public benchmarks, i.e., PROTEINS, NCI1 (Sergey et al., 2020) and FRANKENSTEIN (Orsini et al., 2015), are used in the semi-supervised setting. PROTEINS is a set of proteins that are

classified as enzymes or non-enzymes. NCI1 is a molecular graph set, which is relative to anti-cancer screens where the chemicals are assessed as positive or negative to cell lung cancer. FRANKENSTEIN is molecule dataset for mutagenicity (AMES) classification. The statistics details of these datasets are summarized in Tab. 3. Additionally, for pre-training, the epoch number is set as 1000 and the learning rate is set as 0.0003. During fine-tuning, the label rate is set as 50%. We conduct experiments across various train/test splits in the downstream tasks, repeating them 50 times to derive the mean and standard deviation of the results.

Table 4. Dataset statistics for transfer learning

Utilization	Datasets	#Graphs	#Avg. Nodes	#Avg. Edges	#Features	#Classes	#Tasks
Pretraining	ZINC15	200,000	23.1	24.8	120	0	0
Finetune	Tox21	7,831	18.6	38.6	9	2	12
	ToxCast	8,597	18.7	38.4	9	2	617
	BBBP	2,050	23.9	51.6	9	2	1
	BACE	1,513	34.1	73.7	9	2	1
	SIDER	1,427	33.6	70.7	9	2	27
	ClinTox	1,484	26.1	55.5	9	2	2

Transfer Learning Setting. Following our semi-supervised learning experiments, we proceed to conduct experiments in a transfer learning setting (Hu et al., 2020). We utilize 200,000 unlabeled molecules sampled from the ZINC15 dataset (Sterling & Irwin, 2015) for pre-training, and involve 6 public molecular graph classification benchmarks in the downstream tasks. The statistics details of these datasets are summarized in Tab. 4. Especially, given that Tox21, ToxCast, SIDER, and ClinTox encompass multiple tasks, we compute the final IP Gap and IP ROC for these datasets by averaging the IP Gap and IP ROC across their respective tasks. During pre-training on ZINC15, the epoch number is set as 200 and the learning rate is 0.001. The label rate in fine-tuning is set as 50%. Similar to the learning setting of semi-supervised learning, we conduct experiments across various train/test splits in the downstream tasks for 10 times and report the average and standard deviation of the results.

D.2. Details of Baselines

In this section, we present the details of four state-of-the-art watermarking methods as baselines to protect the IP of the pretraining of GNNs:

- **Deepsign** (Rouhani et al., 2018): This is a watermarking-based method for protecting the ownership of deep learning models in the image domain. The main idea is to ensure the watermark samples to have the same embeddings. During the verification phase, this method requires to access to the intermediate representation of the piracy model. For a watermarked model, the embeddings of watermark samples will be similar, resulting to the same predictions from the downstream classifier. Hence, to extend Deepsign to the black-box verification, the fraction that watermark samples are predicted as the same class is used for IP indication score.
- **RWM-Pre** (Zhao et al., 2021): This baseline is inspired by RWM (Zhao et al., 2021), which focuses on prompting watermarked models to predict Erdos-Renyi (ER) random graphs with random node features and labels to certain classes. Given that RWM is primarily designed for node classification in semi-supervised learning, in order to adapt it to our GNN pretraining scenario, we pretrain a GIN encoder to learn representations. Then, we apply a clustering algorithm to these learned representations, using the resulting cluster labels as pseudo classes for RWM. This approach is denoted as RWM-Pre. During the verification phase, RWM-Pre will compute the fraction of watermark graphs predicted as the same class, serving as the IP indication score.
- **CWM-Pre** (Bansal et al., 2022): This is a certifiable watermarking method to provide watermark certification by injecting noises to model parameters during the watermarking. This method is based on (Zhang et al., 2018) which predicts special samples as certain class. Therefore, to adapt this method for watermarking GNN pretraining, we incorporate the noise injection technique from (Bansal et al., 2022) into RWM-Pre, establishing the baseline as CWM-Pre.
- **GCBA** (Zhang et al., 2023): It is a backdoor attack method for graph contrastive learning. In our setting, we apply the poisoning-based GCBA that aims to align the embeddings of trigger-attached graphs to those of the target class. To evaluate the IP performance of GCBA, we follow the setting in (Adi et al., 2018) to quantify the difference between the

attack success rate of trigger-attached graphs and the classification accuracy of the clean test graphs, both before and after backdooring. These metrics are referred to as the IP Gap and accuracy, respectively, as detailed in Sec. 4.1.

D.3. Implementation Details

In this paper, we follow the settings in (Hu et al., 2020), where we initially train the GNN encoders using GCL or other pretraining methods (Hu et al., 2020). Then, following (Hu et al., 2020), we employ the obtained embeddings to train and evaluate a classifier for the downstream tasks. A 2-layer GIN is deployed as the backbone GNN encoder. The hidden dimension is set as 256 for all experiments. GraphCL is set as the target GCL methods, which is implemented based on PyGCL library (Zhu et al., 2021). The edge prediction and edge masking strategies are implemented based on the source code published by the original authors ¹. The hyperparameter settings of the pretraining are the same as the cited paper.

In the watermark graph pair generation, the probability of connecting each pair of nodes is set as 0.2. We maintain a consistent difference of 15 nodes in the node count between watermark graphs within each pair. By leveraging the randomness in synthetic structures and varying the sizes of the graphs, we are able to generate distinct synthetic graphs to build multiple pairs watermark graphs. In the watermarking loss, the Q and m in Eq.(2) are set as 256 and 1.0.

In experiments of PreGIP, we configure the number of watermark graph pairs as 20 and set $\lambda = 1$, $\epsilon = 2$. To make fair comparisons, all the hyperparameters of these methods are tuned based on the watermarking loss and the pretraining loss on validation set. All models undergo training on an A6000 GPU with 48G memory.

E. Additional Results of Watermarking Pretraining

E.1. Hyperparameter Analysis

We further investigate how hyperparameters λ and ϵ affect the performance of PreGIP, where λ controls the contributions of the proposed watermarking loss on the pretrained models, and ϵ controls the magnitude of changes to the model parameters θ in finetuning-resist watermark injection. More specifically, we vary λ and ϵ as $\{0.01, 0.1, 1, 5, 10\}$ and $\{0.1, 1, 2, 5, 10\}$, respectively. We report the IP ROC and accuracy on PROTEINS datasets. The experimental setting is semi-supervised under the finetuning scenario. All other settings are the same as Appendix D.3. Similar trends are also observed on other datasets and pretraining methods. The results are shown in Fig. 6. From this figure, we find that IP ROC will increase with the increasing of λ and ϵ . As for the accuracy of the watermarked GNN encoder in downstream tasks, it will firstly stay consistent then decrease if the λ and ϵ is overly high. From this figure, we can find that when the ϵ is set around 2 and λ ranges from 0.1 to 1, we can achieve the balance between the GNN encoder utility and watermarking performance. Specifically, according to the hyperparameter analysis on PROTEINS, we set ϵ and λ as 2 and 1. Then, the same hyperparameter setting is applied for all other datasets and experimental settings without further tuning.

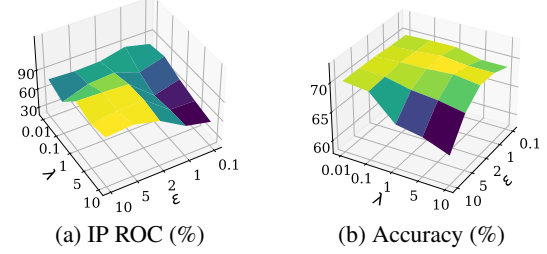


Figure 6. Hyperparameter analysis on PROTEINS.

¹<https://github.com/snap-stanford/pretrain-gnns>

E.2. Additional Results of Flexibility of Watermarking

The full comparison results are reported in Tab. 5. The observations are rather similar to those of Fig. 3 in Sec. 4.2.

Table 5. Results in protecting IP of edge prediction-pretrained GNNs (Hu et al., 2020) in the semi-supervised setting.

Scenario	Dataset	Metrics (%)	Non-Watermarked	Deepsign	RWM-Pre	CWM-Pre	PreGIP
Fix	PROTEINS	Accuracy	68.0 \pm 1.1	66.6 \pm 1.4	62.3 \pm 1.2	62.9 \pm 0.9	69.1\pm1.1
		IP Gap	-	6.0 \pm 4.7	29.5 \pm 9.7	8.1 \pm 2.5	31.0\pm3.5
		IP ROC	-	34.5	90.0	58.0	100
	NCI1	Accuracy	68.7 \pm 0.9	69.0 \pm 1.0	68.4 \pm 0.8	68.5 \pm 0.8	69.7\pm0.6
		IP Gap	-	7.5 \pm 0.1	12.5 \pm 1.3	11.0 \pm 2.3	43.0\pm9.8
		IP ROC	-	84.0	78.0	82.5	100
Finetune	PROTEINS	Accuracy	68.2 \pm 1.5	68.2 \pm 2.2	67.5 \pm 1.6	63.1 \pm 3.1	67.9\pm2.2
		IP Gap	-	3.0 \pm 1.0	6.0 \pm 5.0	14.0 \pm 7.5	35.0\pm1.4
		IP ROC	-	54.0	61.0	58.5	87.5
	NCI1	Accuracy	69.6 \pm 0.8	68.8 \pm 0.8	69.7 \pm 0.9	69.7 \pm 0.6	70.8\pm0.9
		IP Gap	-	4.5 \pm 0.7	5.0 \pm 1.5	9.5 \pm 3.4	16.5\pm14.7
		IP ROC	-	43.0	60.5	68.0	85.0

E.3. Additional Results of Pretraining for Transfer Learning

The comparison results of the edge masking pretraining on 6 downstream datasets are reported in Tab. 6. The observations are rather similar to those of Tab. 2 in Sec. 4.2.

Table 6. Comparison with baselines in protecting IP of edge masking-pretrained GNNs in the transfer learning setting.

Dataset	Metrics (%)	Non-Watermarked	Deepsign	RWM-Pre	CWM-Pre	PreGIP
Tox21	Accuracy	92.7 \pm 0.2	92.8 \pm 0.1	92.9 \pm 0.2	92.8	92.9\pm0.2
	IP Gap	-	4.9 \pm 11.6	7.5 \pm 4.8	11.9 \pm 10.6	32.4\pm28.0
	IP ROC	-	38.0	62.0	66.0	96.0
ToxCast	Accuracy	83.5 \pm 0.3	83.7 \pm 3.2	83.4 \pm 0.4	83.3 \pm 0.1	83.8\pm0.1
	IP Gap	-	4.4 \pm 3.2	27.6 \pm 24.6	7.2 \pm 2.4	33.6\pm12.1
	IP ROC	-	96.0	72.0	70.0	100.0
BBBP	Accuracy	83.9 \pm 1.8	85.5\pm1.1	85.3 \pm 1.2	85.2 \pm 1.1	85.4 \pm 1.4
	IP Gap	-	12.0 \pm 6.8	25.4 \pm 22.0	26.1 \pm 12.0	39.0\pm30.5
	IP ROC	-	90.0	80.0	84.0	94.0
BACE	Accuracy	70.2 \pm 0.8	73.4 \pm 2.2	74.3 \pm 1.8	74.4 \pm 1.6	74.5\pm2.4
	IP Gap	-	6.7 \pm 6.4	26.7 \pm 25.9	12.2 \pm 10.4	38.0\pm26.4
	IP ROC	-	68.0	80.0	78.0	84.0
SIDER	Accuracy	75.3 \pm 0.3	75.1\pm0.3	74.8 \pm 0.4	74.7 \pm 0.3	74.8 \pm 0.2
	IP Gap	-	3.7 \pm 3.4	27.8 \pm 27.1	21.4 \pm 17.5	31.2\pm29.6
	IP ROC	-	20.0	80.0	64.0	80.0
ClinTox	Accuracy	91.3 \pm 0.5	91.6 \pm 1.2	91.6 \pm 1.7	91.4 \pm 1.3	91.8\pm1.2
	IP Gap	-	2.0 \pm 1.0	37.2 \pm 34.0	33.2 \pm 31.5	45.0\pm42.0
	IP ROC	-	40.0	82.0	80.0	86.0

E.4. Additional Results of Impact of the Number of Watermark Graph Pairs

The IP ROC results of PreGIP on PROTEINS and FRANKENSTEIN are reported in Tab. 7. The observations are rather similar to those of Fig. 4 in Sec. 4.3.

Table 7. IP ROC of PreGIP under different numbers of watermark graph pairs (%).

Dataset	1	5	10	20	50	100
PROTEINS	55	92.5	96.5	100	100	100.0
FRANKENSTEIN	50	90	100	100	100	100.0